NJC

Accepted Manuscript

This is an *Accepted Manuscript*, which has been through the Royal Society of Chemistry peer review process and has been accepted for publication.

Accepted Manuscripts are published online shortly after acceptance, before technical editing, formatting and proof reading. Using this free service, authors can make their results available to the community, in citable form, before we publish the edited article. We will replace this *Accepted Manuscript* with the edited and formatted *Advance Article* as soon as it is available.

You can find more information about *Accepted Manuscripts* in the Information for Authors.

Please note that technical editing may introduce minor changes to the text and/or graphics, which may alter content. The journal's standard Terms & Conditions and the Ethical guidelines still apply. In no event shall the Royal Society of Chemistry be held responsible for any errors or omissions in this *Accepted Manuscript* or any consequences arising from the use of any information it contains.

ROYAL SOCIETY OF CHEMISTRY

www.rsc.org/njc

Cite this: DOI: 10.1039/c0xx00000x

www.rsc.org/xxxxxx

ARTICLE TYPE

Evaluation of an efficient and selective adsorbent based on multi-walled carbon nanotubes coated silica microspheres for detecting nucleobases and nucleosides in human urine

Xiaoming Sun[a], Yanan Tang[b,a] Duolong Di*[a], Mei Guo[b] and Lei Zhao[b]

Received (in XXX, XXX) Xth XXXXXXXXX 20XX, Accepted Xth XXXXXXXXX 20XX
DOI: 10.1039/b000000x

Multi-walled carbon nanotubes (MWCNTs) can be used in analytical chemistry for separation and purification and offer the opportunity to determine low concentration compounds in complex system. The novel multi-walled carbon nanotubes coated silica microspheres (MWCNTs/SiO_2) were synthesized by covalent binding of amido bond. The characteristics results from emission scanning electron microscope (SEM), transmission electron microscope (TEM), fourier transformed infrared spectrometer (FTIR) and Brunauer-Emmett-Teller (BET) showed that MWCNTs/SiO_2 was successfully prepared. By evaluating the static adsorption capacities of ten nucleobases and nucleosides, the adsorption of microspheres for adenine (A), guanine (G), uric acid (UA) and xanthosine (X) were significantly stronger than the others. Moreover, the adsorption capacity depends on the pH value, salinity and contact time. It was shown that π–π conjugation and hydrogen bonding interactions were the two main driving forces for the adsorption of target compounds. Adsorption kinetics and adsorption isotherm showed that the adsorption process was a chemical and multilayer adsorption. They could be determined within the test ranges with a good correlation coefficient ($r > 0.997$). The limits of detection (LOD) for A, G, UA and X were 1.22, 2.02, 0.32 and 2.28 ng/mL, respectively. The intra- and inter-day relative standard deviations (RSD) were no more than 6.5%. This procedure therefore afforded a convenient, sensitive and accurate method with a high extraction efficiency for the determination of A, G, UA and X in human urine.

Introduction

The nucleobases, nucleosides and their metabolites play an important role in the process of cell proliferation and metabolism, which could be found in biological fluids, such as urine, serum and cerebrospinal fluid. They also have a lot of physiological activities including anticonvulsant activity, stimulating axon growth in vitro and in the adult central nervous system, influencing the growth and differentiation of the gastro intestinal tract, and maintaining the immune response.[1] Concentrations of nucleosides in urine and serum are mostly very low with the exception of uridine and uric acid, and raised concentrations in plasma and urine can be used as biomarkers in some diseases, such as diabetes, gout and cancer.[2-4] Thus, the separation and detection of nucleobases and nucleosides is an interesting and challenging task and is much more important in biomedical area. To quantify the nucleobases and nucleosides, biological fluids could be concentrated by vacuum drying under low temperature, freeze drying and/or drying under nitrogen. However, these methods will be a time consuming process and depend on the special instrument. During the last decade, many analytical methods for measuring and monitoring nucleosides in biological fluids have been reported, such as solid phase extraction (SPE) combined with high performance liquid chromatography (HPLC), ultra-sensitive LC–MS/MS and capillary electrophoresis (CE) methods.[5-9]

Generally, the SPE method is used in detecting analytes on trace level and the performance often depends on the property of adsorbents. In order to increase the sensitivity and selectivity in nucleosides analysis, some new adsorbents have been synthesized and characterized to improve the detection sensitivity (i.e. water-holding adsorbents bonded with a zwitter-ionic polymer[10], online affinity solid phase extraction[11], graphene[12], molecularly/ion imprinted polymer[13-15]). Nowadays, nanomaterial show more impressive characteristics compared with non-nanomaterial, such as large specific surface areas, high tensile strength, high thermal conductivity and stability, etc. Thus, the sample separation and pre-concentration techniques based on nanomaterials play important roles in the increase of analytes concentration and the removal of interfering species. As solid adsorbents, carbon nanotubes (CNTs) in SPE for the determination of inorganic and organic compounds have considerably increased. The inorganic ions of Cd(II), Co(II), Ni(II) and Zn(II) in various samples (i.e. lichen, bovine liver, river sediment, pharmaceuticals, food and water) were determined using CNTs as SPE adsorbent.[16-18] The obtained pre-concentration factor was 100, and satisfied results were achieved when the method was used for the determination of these ions in real water samples and a reference material. In

addition, CNTs have been successfully used as SPE adsorbents for the extraction of different families of pesticides[19], pharmaceuticals[20], phthalate esters, phenolic compounds and others[21-23].

In this paper, a new method based on SPE was developed for the analysis of nucleobases and nucleosides in urine. Multi-walled carbon nanotubes (MWCNTs) coated silica microspheres (MWCNTs/SiO_2) by using covalent decoration of amino bond was synthesized, which could avoid the easily agglomeration of MWCNTs. MWCNTs can be deposited onto the surface of a chromatographic solid phase to generate a packing material[24-27] and the adsorption character was improved. The extraction protocol was successfully applied to directly and selectively extract adenine (A), guanine (G), uric acid (UA) and xanthosine (X) from human urine. Meanwhile , the adsorption mechanism had been interpreted by the adsorption kinetics and adsorption isotherm and which proved that this SPE protocol suited for the quick detection of nucleobases and nucleosides in human urine.

Expetimental

Chemicals and materials

Silica microspheres (5 μm particle size, 70 Å pore diameter and 360 m^2g^{-1} specific surface areas) were synthesized using the polymerization induced colloid aggregation method by 501 research group in our institute. Multi-walled carbon nanotubes (ID: 2-5 nm; OD: < 8 nm; Length: 0.5-2.0 μm; SSA: > 500 m^2/g) were obtained from Chengdu Organic Chemicals Co., Ltd, Chinese Academy of Sciences. Analytical grade 3-aminopropyltriethoxysilane was purchased from Sun Chemical Technology Co., Ltd.. A, G, UA, X and other nucleobases and nucleosides were purchased from Yacoo Chemical Reagents Co., Ltd.. Toluene, thionyl chloride, tetrahydrofuran, dichloromethane, ethanol, methanol, acetone, sulfuric acid, nitric acid and hydrochloric acid were of analytical grade and obtained from various commercial sources. Deionized water was purified with a water purified system, which was purchased from Res. J Scientific Instruments Co., Ltd. and used for all aqueous solutions.

Analysis and characterization

All HPLC analysis were performed on an Agilent HPLC series 1200 system (Agilent Technologies, Palo Alto, CA), which consisted of G1312A bin pump and G1315B DAD detector. Thermostated column compartment (AT-950) was purchased from Auto Science Technology Co., Ltd (Tianjin, China). A Sino-Chrom ODS-AP analytical column (RP-C18 column 250 mm × 4.6 mm i.d. 5 μm particle size) (Dalian Elite Analytical Instruments Co., Dalian, China) was used for separation. The flow rate was 1.0 mL/min and the column temperature was 30°C unless otherwise specified. The detection wavelength was 260 nm. Mobile phases were prepared by mixing 0.2% acetic acid water solution (A) and methanol (B). The gradient elute was performed as follows, 0-5 min, 5% (B); 5-10 min, 5-15% (B).

The surface morphologies of bare SiO_2 and MWCNTs/SiO_2were conducted on a JSM-6701F field emission scanning electron microscope (SEM) (Hitachi, Japan) and TECNAI G^2 transmission electron microscope (TEM) (FEI, USA). Fourier transformed infrared (FTIR) spectra of bare SiO_2, 3-aminopropyl silica microspheres and MWCNTs/SiO_2 were examined on a Nexus 870 spectrometer (Nicolet, USA) in the range of 4000-400 cm^{-1}. SHA-B incubator (Jintan Zhengji Instrument Co., Ltd., China) was used for adsorption experiments. The specific surface area, pore volume, and pore size distribution of the adsorbents were calculated via the nitrogen adsorption and desorption curves at 77 K according to Brunauer-Emmett-Teller (BET) and Barret-Joyner-Halenda (BJH) methods and using a Micromeritics ASAP2020 automatic surface area and porosity analyzer (Micromeritics Instrument Corp., Atlanta, GA, USA), respectively.

Synthesis of MWCNTs/SiO_2

In order to activate the silanol group, 2.5 g of silica microspheres was dispersed in 100 mL of 20% HCl and stirred at 100°C for 4 h, then washed by deionized water to remove Cl^-, and finally dried at 80°C. Then, 30 mL of 3-aminopropyltriethoxysilane was slowly dropped into the suspension of dry toluene which contained silica microspheres. The mixture was stirred at 100°C for 8 h under reflux. Finally, 3-aminopropyl silica microspheres (APGS) were obtained by filtering and subsequent washing for several times by dry toluene and acetone. MWCNTs (0.5 g) were immersed into 60 mL of HNO_3:H_2SO_4 (1:3, v/v) solution for 6 h under stirring at 80°C, and thereafter vacuum-filtered through a 0.22 μm millipore polytetrafluoroethylene membrane and washed with distilled water until the MWCNTs have become neutral. After drying under vacuum at 70°C, the product MWCNTs-COOH was obtained. Then MWCNTs-COOH were suspended in 20 mL of $SOCl_2$ solution in an ultrasonic bath for 30 min and then stirred at 85°C for 6 h. MWCNTs-COCl was prepared by filtering and washing with $CHCl_3$ for several times. Certain amount of MWCNTs-COCl (25 mg) in THF was sonicated for 30 min before the addition of APGS (7.5 g). This mixture was stirred at 80°C for 6 h under reflux and then washed several times with THF followed by ethanol.[24-27]

Preparation of sample solution

The standard solutions of A, G, UA and X were diluted by water and the pH value was adjusted to 7 by 0.04 mol/L NaOH solution. The urine sample was collected and centrifuged at 10000 rpm for 10 min. The supernatant was stored at 4°C and then filtered through a 0.22 μm millipore filter before analysis. With permission, all procedures involving sample collection and analysis were carried out according to the guidelines of the institutional ethical committee (Lanzhou Institute of Chemical Physics, CAS and Gansu College of Traditional Chinese Medicine). In this study, informed consent to participate was given by all subjects.

Static adsorption experiments

The static adsorption experiment was performed by three steps. (1) 30 mg MWCNTs/SiO_2 were added to the mixed standard solution and were shaken for 15 s. (2) The mixture was continually shaken in an incubator (100 rpm) at 30°C for 2 h. (3) The mixture was centrifuged at 10000 rpm for 10 min to isolate MWCNTs/SiO_2 adsorbents. Then the raw standard solution and adsorption residue were determined by HPLC.

Dynamic adsorption experiments

Pipette tips were used as the SPE cartridges and were prepared by packing with 50 mg MWCNTs/SiO_2. An upper and lower degreasing cotton were used to avoid the loss of adsorbents. Prior to extraction, the adsorbents were packed in the pipette tips and were sequentially washed with 1.0 mL of methanol and 1.0 mL of water. Then 1.0 mL of sample solution with 20% NaCl (m/v) was passed through the SPE pipette tips. Analytes were desorbed by 200 μL of NaOH-methanol-water (pH 8) solution and dried under nitrogen. The residual was redissolved by 100 μL of water (pH 8). Finally, the raw standard solution, the adsorption residue and redissolved solution were determined by HPLC.

Adsorption Isotherm

The solutions (50 mL) with different concentrations of A, G, UA and X (C_0 = 0.5, 1.0, 2.0, 4.0, 6.0, and 8.0 μg/mL) were contacted with pretreated MWCNTs/SiO_2 (0.1 g) in conical flasks. The flasks were continually shaken for 4 h at temperatures of 298.15, 308.15, and 318.15 K, respectively. Then, the concentrations of the adsorption solutions were analyzed by HPLC.

Results and discussion

Characterization of MWCNTs/SiO_2

The topography of bare SiO_2 and MWCNTs/SiO_2 surface were characterized by SEM and TEM (Figure 1). The surface topography of bare SiO_2 microspheres was smooth and compact. After MWCNTs had been coated, the surface was rough and the tubular structure of MWCNTs could been observed clearly. Figure 2 shows the FTIR spectra of pristine SiO_2, APGS and MWCNTs/SiO_2. The bands in 1100 cm^{-1} and 3400 cm^{-1} region were respectively attributed to Si–O–Si and –OH stretching on silica surface. The bands in 1570 cm^{-1} and 1670 cm^{-1} region were assigned to C=O stretching of amide bond. For the amide bond, the strong stretching of –NH could also be observed in 1100 cm^{-1}.The bands around 3000 cm^{-1} region were attributed to $–CH_2–$ and C=C stretching. The spectra therefore certify that MWCNTs had been successfully grafted on the silica microsphere through the silane and amide bonds.

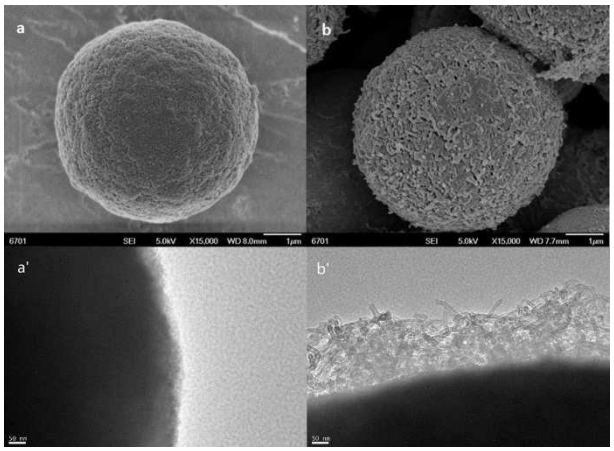

Figure 1: SEM and TEM micrographs of adsorptions.SEM: bare silica microspheres (a) and MWCNTs/SiO_2 (b); TEM: bare silica microspheres (a') and MWCNTs/SiO_2 (b')

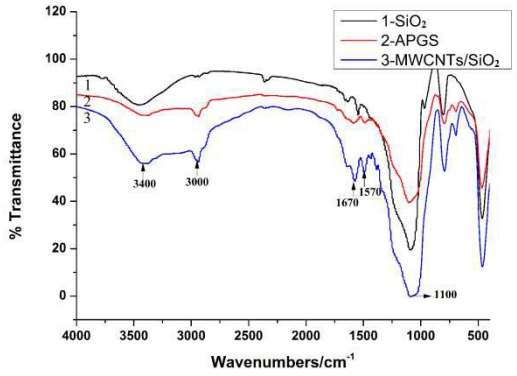

Figure 2: FTIR spectra of pristine silica microspheres, APGS and MWCNTs/SiO_2. 1: SiO_2; 2: APGS; 3: MWCNTs/SiO_2.

Nitrogen adsorption/desorption measurements were performed and the adsorption/desorption isotherms of MWCNTs/SiO_2 can be observed from Figure 3. The MWCNTs/SiO_2 microspheres were mainly mesoporous according to the International Union of Pure and Applied Chemistry (IUPAC) nomenclature. As shown in Table 1, the surface area, total pore volume, and average pore diameter of pristine SiO_2 and MWCNTs/SiO_2 were obtained by the standard BJH adsorption cumulative method. After MWCNTs had been covalent decorated on the SiO_2 surface, MWCNTs may partly penetrate into and block the pores of SiO_2 microspheres. Therefore, the surface area, total pore volume, and average pore diameter were smaller than the pristine SiO_2.

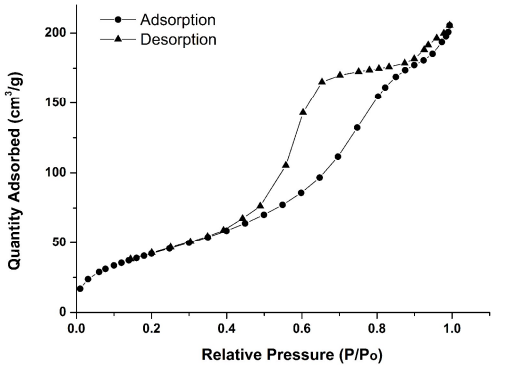

Figure 3: Nitrogen adsorption/desorption isotherms of MWCNTs/SiO_2 microsphere.

Table 1 Specific surface area, total pore volume, andaverage pore diameter of pristine SiO_2 and MWCNTs/SiO_2 microsphere.

	BET surface area (m^2/g)	pore volume (cm^3/g)	porediameter (nm)
pristine SiO_2	360	0.9	9.1
MWCNTs/SiO_2	160	0.3	7.5

Adsorption mechanism

Adsorption capacities were studied to further investigate the adsorption differences of the four compounds. From Figure 4, six concentration gradients were considered and the adsorption capacity of UA is strongest and X is weakest. Compared with the other three compounds, X contains a carbohydrate so that the

steric hindrance resulted in fewest adsorptions on MWCNTs. The π–π conjugation was considered as the main interactions between nucleobases and nucleosides and MWCNTs. Therefore adsorption intensity of X is weakest because of the shorter conjugated system. Each of UA, A and G compound contains four π bonds which form a complete conjugated system. However, UA is easier to form a flat structure without the interference of $–NH_2$ group. Therefore, conjugated system of UA is easy to interact with π–π conjugation on MWCNTs. In addition, three carbonyls groups also make UA a multi-points compound to act with residual –COOH to form hydrogen bond on MWCNTs. Compared with A, G contains a carbonyls group, a $–NH_2$ group and two –NH– groups, which are all reaction points of π–π interaction and hydrogen bond. Therefore, at the same concentration, adsorption capacity of G is stronger than that of A. In addition, Akdim et al. showed that the trend of adsorption energies was G > A by density functional theory calculations.[28]

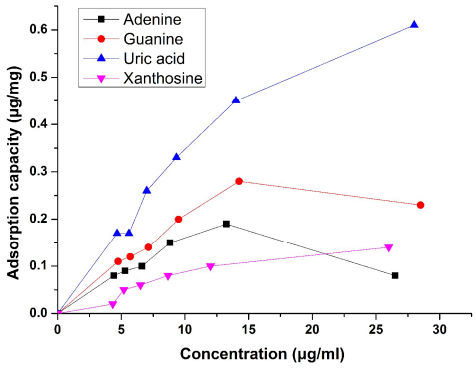

Figure 4: The adsorption capacities of A, G, UA and X.

The adsorption differences could be elucidated by the main chemical interaction of π–π conjugations and hydrogen bond actions. For the interaction between nucleic acid bases and CNTs, Wang indicated that in addition to noncovalent π-π interactions between the adenine base of dinucleoside and CNT, hydrogen bond interactions also develop between the sugar residue and the π orbital of CNTs.[29] To further evaluate the adsorption capacity and to verify the applicability of adsorbents in SPE mode, the adsorption capacities of some other nucleobases and nucleosides were also investigated. As shown in Figure 5, under the same adsorption condition, uracil, xanthine, hypoxanthine, uridine, inosine and guanosine could not be adsorbed on the surface of MWCNTs.

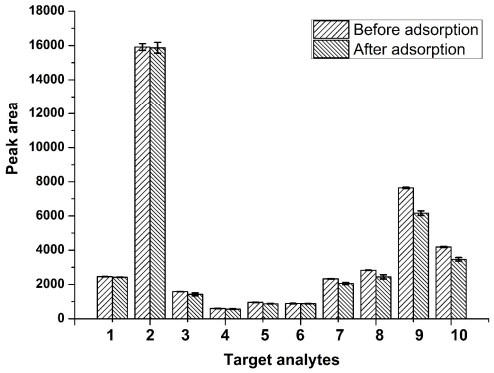

Figure 5: Adsorption characters of ten nucleobases and nucleosides. (The concentration are as follows, 1. uracil: 0.07 mg/ml; 2. xanthine: 0.27 mg/ml; 3. hypoxanthine: 0.05 mg/ml; 4. uridine: 0.03 mg/ml; 5. inosine: 0.07 mg/ml; 6. guanosine: 0.04 mg/ml; 7. guanine: 0.04 mg/ml; 8.adenine: 0.06 mg/ml; 9.xanthosine: 0.17 mg/ml; 10. uric acid: 0.22 mg/ml).

Adsorption Kinetics of A, G, UA and X

Pseudo-first-order and pseudo-second-order kinetics models were calculated and applied to better illustrate the adsorption mechanism of A, G, UA and X onto MWCNTs/SiO_2. The equations are presented as follows:

Pseudo-first-order kinetics model:

$$\ln(q_e - q_t) = \ln q_e - k_1 t \quad (1)$$

Pseudo-second-order kinetics model:

$$\frac{t}{q_t} = \frac{1}{k_2 q_e^2} + \frac{1}{q_e} t \quad (2)$$

where q_e and q_t are the adsorption capacity for A, G, UA and X onto the MWCNTs/SiO_2 at equilibrium and at any time t (mg/g), respectively. The parameters k_1 (1/min) and, k_2 (g/(mg min)) are the rate constants of the models for the adsorption process.

Corresponding parameters and fitting equations were listed in Table 2. Compared with experimental results, the values of q_e and

Table 2 Kinetics parameters for the adsorption of A, G, UA and X onto MWCNTs/SiO_2

	A			G		
	Linear equation	k	R^2	Linear equation	k	R^2
M 1[a]	$\ln(0.008-q_t)$= -0.013t+2.063	0.013	0.508	$\ln(0.028-q_t)$= -0.026t+3.326	0.026	0.976
M 2	t/q_t= 38.74t+482.6	3.109	0.989	t/q_t= 19.10t+316.0	1.154	0.991
	UA			X		
	Linear equation	k	R^2	Linear equation	k	R^2
M 1	$\ln(0.085-q_t)$= -0.027t+4.443	0.027	0.831	$\ln(0.023-q_t)$= -0.024t+3.125	0.024	0.734
M 2	t/q_t= 2.990t+17.22	0.519	0.999	t/q_t= 31.44t+863.9	1.144	0.972

[a] M1: Pseudo-first-order kinetics model; M2: Pseudo-second-order kinetics model

R^2 for the pseudo-second-order model were much more reasonable than that of the pseudo-first-order model. Therefore,

the adsorptions of A, G, UA and X onto the MWCNTs/SiO_2 fitted to the pseudo-second-order model, and was applied for the entire process. The principle of pseudo-second-order model kinetics assumed that the rate-limiting step might be the adsorption, in agreement with chemical adsorption being the rate-controlling step, in which concentrations of both adsorbate and adsorbent were involved.[30] So, the adsorption of A, G, UA and X onto the MWCNTs/SiO_2 might be chemical adsorption. This might be agreement with the analysis in the previous section.

Adsorption Isotherms of A, G, UA and X

The equilibrium adsorption isotherms of A, G, UA and X from aqueous solution onto MWCNTs/SiO_2 were obtained at 298.15 K, 308.15 K and 318.15 K, respectively. Generally, the adsorption isotherm is the functional expression of the relationship between the adsorbate and the amount of solid adsorbent at a given temperature under equilibrium conditions. The most widely used isotherm models are Langmuir and Freundlich isotherms.

The Langmuir isotherm model was originally developed to describe chemisorptions on a group of localized adsorption sites and have been used for many adsorption process of monolayer solid-liquid adsorption. The equation is represented as:

$$C_e / q_e = K_L / q_m + C_e / q_m \quad (3)$$

where q_e and q_m are the equilibrium and maximum adsorption capacity (mg/g), respectively. C_e is the equilibrium concentration of A, G, UA and X solution (mg/mL). K_L is the parameter related to the adsorption energy (mg/mL).

The Freundlich isotherm equation is derived to model the multilayer and heterogeneous surface adsorption. The equation is expressed as:

$$\lg q_e = (1/n)\lg C_e + \lg K_F \quad (4)$$

where K_F reflects the adsorption capacity of an adsorbent ((mg/g)(mL/mg)$^{1/n}$). The parameter n represents the adsorption affinity of the adsorbent for an adsorbate. The parameters qe and Ce are the same as mentioned above. [31]

The parameters of corresponding isotherms are list in Table 3.

Table 3 Parameters of Langmuir and Freundlich isotherm models

	Temperature (K)	Langmuir isotherm model	R^2	Freundlich isotherm model	R^2
A	298.15	q_e=0.340Ce/(1.114+Ce)	0.848	lnq_e=0.659lnCe-2.050	0.855
	308.15	q_e=0.169Ce/(0.151+Ce)	0.844	lnq_e=0.931lnCe-2.269	0.913
	318.15	q_e=0.110Ce/(0.444+Ce)	0.699	lnq_e=1.519lnCe-2.211	0.981
G	298.15	q_e=-8.547Ce/(-32.350+Ce)	0.636	lnq_e=1.062lnCe-1.307	0.989
	308.15	q_e=-4.255Ce/(-13.766+Ce)	0.850	lnq_e=1.689lnCe-1.519	0.957
	318.15	q_e=-1.414Ce/(-8.785+Ce)	0.798	lnq_e=0.769lnCe-0.956	0.810
UA	298.15	q_e=0.304Ce/(3.695+Ce)	0.958	lnq_e=2.102lnCe-4.779	0.992
	308.15	q_e=0.525Ce/(2.029+Ce)	0.979	lnq_e=0.809lnCe-1.796	0.903
	318.15	q_e=0.764Ce/(1.661+Ce)	0.939	lnq_e=0.733lnCe-0.973	0.838
X	298.15	q_e=0.543Ce/(11.374+Ce)	0.945	lnq_e=1.410lnCe-4.078	0.958
	308.15	q_e=0.295Ce/(5.573+Ce)	0.942	lnq_e=1.238lnCe-3.533	0.903
	318.15	q_e=0.397Ce/(8.662+Ce)	0.944	lnq_e=1.121lnCe-3.664	0.881

Regression analysis showed that the Freundlich isotherm was a better model compared with Langmuir isotherm, which means the adsorption of A, G, UA and X was a multilayer adsorption. The value of 1/n was a measure of adsorption intensity. The value of 1/n below 1 demonstrated favourable adsorption, and above 1 was indicative of cooperative adsorption. Not all the values of 1/n were in the range of 0-1, which indicated that there are some competitive adsorptions among A, G, UA and X.

Effect of contact time

The process of dynamic equilibrium depends on partitioning of the target analytes between adsorption solvent and adsorbents. The mass transfer is therefore a time-dependent process. In order to determine highest point when arriving at extraction equilibrium, the extraction time was firstly investigated. As shown in Figure 6, the adsorption capacity which was expressed by peak area increased by increasing the extraction time from 0 to 30 min. The adsorption capacity slowly decreased from 30 to 60 min, and then it reached equilibrium slowly after 60 min. According to the conjugate structure of four compounds, the acting force between compounds and MWCNTs/SiO_2 may be mainly ascribed to the π-π conjugation, amido bond and hydrogen bond. If the acting point were occupied, excess analytes could not be adsorbed onto the surface of MWCNTs/SiO_2. Therefore, as time goes on, no more compounds would be adsorbed after 30 min and some may be desorbed into the solution.

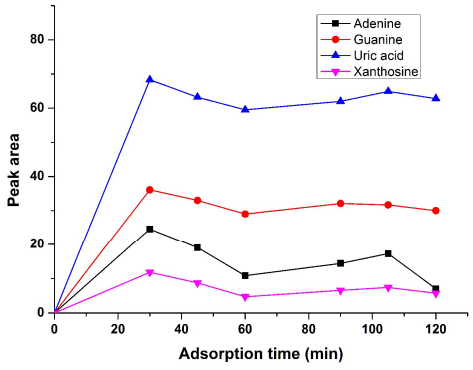

Figure 6: Effect of extraction time on the extraction efficiency. Sample solution, 2 mL of aqueous solution containing 2.5 μg/mL of A, 2.0 μg/mL of G,10.4 μg/mL of UA and 10 μg/mL of X. Extraction temperature was 30 ºC; stirring speed was 100 rpm without addition of salt.

Effect of pH value of the sample solution

In SPE, mass transfer is promoted by the optimal pH conditions in sample solution. The pH value of the sample solution should suppress analytes ionization to keep the molecular form. Besides, all the four compounds could not easily dissolve in water without adding acid or base. Therefore, some water solution (pH 3 ~ 9) were prepared. It can be seen from Figure 7 that the adsorption capacity of A and G increased slowly when the solution pH changing from 3 to 6 and decreased when the solution pH changing from 7 to 9. UA and X reach a relative high adsorption capacities when pH value is 6. Thus the solution pH for SPE study was selected as 6~7, considering the solubility under the basic environment.

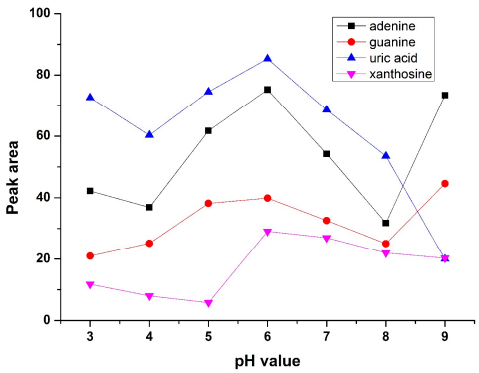

Figure 7: Effect of sample pH on the extraction efficiency of A, G, UA and X extracted with MWCNTs/SiO_2-SPE. Sample solution, 3 mL of aqueous solution containing 4.2 μg/mL of A, 3.3 μg/mL of G, 17.3 μg/mL of UA and 16.8 μg/mL of X.

Effect of the desorption solvent

Other critical factors which affect the extraction efficiency are the type and volume of elute used for removing analytes from adsorbents. For desorption of the four compounds, six kinds of solvents including methanol, acetonitrile, acetone, ethyl acetate, NaOH-methanol-water (pH 8) and HCl-methanol-water (pH 3) were evaluated. The compounds of A, G, UA and X could be desorbed only by acetone and NaOH-methanol-water (pH 8) solution. The desorption efficiencies (DE; DE = C_{elute} /($C_{original}$-$C_{dsorption}$)) of A, G, UA and X eluted by acetone were 5.6%, 14.0%, 11.2% and 10.5%, respectively. Compared with acetone, the DE of which eluted by NaOH-Methanol-water (pH 8) was 104.1%, 89.7%, 93.5% and 95%, respectively. Thus, desorption solution was chosen as NaOH-methanol-water (pH 8) solution. To improve the sensitivity, desorption volume was chosen as 200 μL and some concentration procedures were performed to avoid the solvent effect of methanol for HPLC analysis.

Effect of salinity

As shown in Figure 8, the adsorption capacity of A, G and UA increased significantly when NaCl concentration in sample solution increased from 1% to 20%. However, the adsorption capacity of X decreased when the NaCl concentration is above 10%. Generally, the addition of salt could lead to an increase of ionic strength in the sample solution which might reduce the solubility of the A, G, X and UA and could accelerate the π-π conjugation between molecule and MWCNTs. Therefore, some added salt would increase the acting force and result an increasing adsorption capacity. In this paper, the NaCl concentration was chosen as 20% to increase the adsorption capacity.

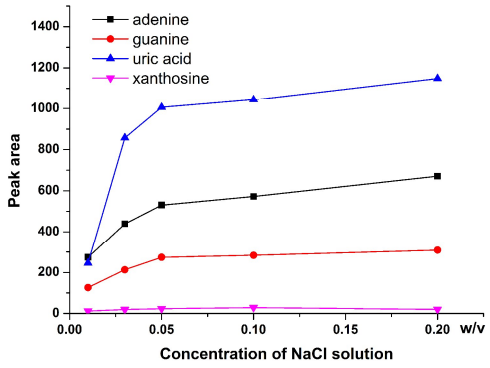

Figure 8: Effect of salt addition to the adsorption efficiency.

Method evaluation

Under the optimized conditions, a series of experiments were performed to determine the linear regression, limit of detection, precision and EF of A, G, UA and X. The working curves were constructed by plotting the peak areas and the concentrations of analytes in a series of spiked sample solutions. The relative standard deviation was obtained by extraction of three replicates at the same time and this extraction was carried out under optimum conditions. A, G, UA and X were extracted with a satisfactory enrichment factor (EF) of 10, 3, 5 and 27, respectively. The linear regression equations, correlation coefficients, LOD, LOQ, EF and RSD are listed in Table 4.

Table 4 The linear regression equations, correlation coefficients, LOD, LOQ, EF and RSD

Analytes	LRE[a]	Linear ranges (μg/ml)	Correlation coefficients	LOD (ng/mL)
A	y=79.23x+30.62	3.1-61.2	0.999	1.22
G	y=3.10x+86.55	25.2-504.0	0.997	2.02
UA	y=13.36x+7.98	0.9-458.0	0.999	0.32
X	y=25.58x+8.35	1.4-28.6	0.999	2.28
	LOQ (ng/mL)	EF	RSD (inter-daily)	RSD (intra-daily)
A	3.44	10	5.4	3.5
G	6.10	3	4.4	2.7
UA	0.98	5	3.2	2.8
X	7.15	27	6.3	4.3

[a] LRE: The abbreviation of linear regression equations.

LOD: limit of detection (S/N=3)

LOQ: limit of quantification (S/N=10)

RSD: relative standard deviation

EF: EF was the concentration ratio of analyte presented in the injection solution to that originally presented in the sample.

EF = $C_{elute\ solution}$ /$C_{sample\ solution}$

Stability of adsorbents

During the extraction process, acid and base solutions were always used. Thus, it is necessary to investigate the stability of MWCNTs/SiO_2 adsorbents under acid and base solutions. In this

experiment, the pH values of acid and base solution were 3 and 10, respectively. MWCNTs/SiO_2 adsorbents were added to the solution and immersed for 24 h, then were washed by water to remove excessive H^+ and OH^-. The standard solution was used to evaluate the performance of absorbents. As shown in Figure 9, compared with the columns of "after adsorption" and "acid/base treatment", no significant changes were observed. Thus, MWCNTs/SiO_2 absorbents were evaluated to be stable after acid or base treatment.

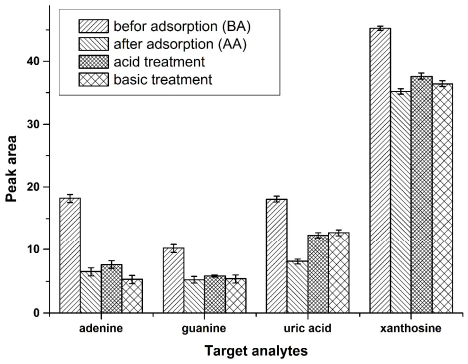

Figure 9: Evaluation of the stability of MWCNTs/SiO_2 adsorbents under acid and/or basic environment.

Analysis of urine samples

Urine sample was collected and determined following the procedure of "Dynamic adsorption experiments". The chromatograms of original and elute sample solution were shown in Figure10. The concentrations of A, G and X in real urine sample were too low to detect, therefore standard solution of 4.10, 11.97, 1.20 μg/mL were added. The recoveries of the four compounds in three added grade (80%, 100%, 120%) were evaluated. From Table 5, the recoveries of four compounds are between 98.06% and 101.67% and the RSD are from 1.76% to 5.97%. The comparison of other methods for the determination of the target nucleoside and nuclebase is shown in Table 6.

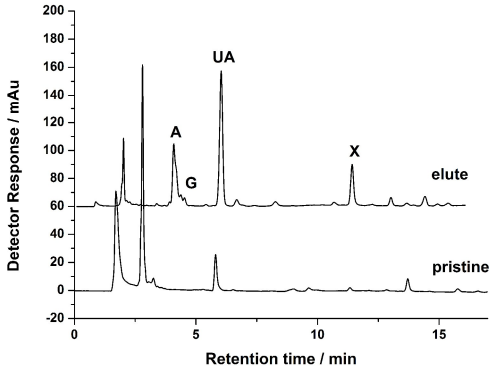

Figure 10: Chromatograms of pristine and elute solution of real urine sample.

Table 5 Recovery of four compounds in urine determined under the optimized conditions

Analytes	original μg/ml	spiked μg/ml	found μg/ml	Recovery %	RSD %
A	4.10	6.24 5.2 4.32	10.21 9.22 8.43	98.37±0.02	1.76
G	11.97	12.05 10.04 8.03	23.95 22.92 19.76	101.67±0.05	5.10
UA	26.31	35.28 29.4 23.52	61.57 55.33 50.54	100.39±0.02	2.10
X	1.20	1.34 1.12 0.89	2.59 2.23 2.06	98.06±0.06	5.97

Table 6 Comparison of other methods for the determination of the target nucleoside and nuclebase

Application	Analytes	Adsorbents	Detection method	LOD(μg/ml)	Ref.
Tuber sample	A G	macroporous resin-DSPE[a]	HPLC-DAD	0.4 0.3	8
urine	X	Affinity-gel-SPE[b]	CE-DAD[c]	0.12	9
urine	G	Boronate affinity magnesia–zirconia composite-SPE	HPLC-DAD	0.005	32
urine	A G	Affinity-gel-SPE	CE-DAD	3.51 (nM) 10.0 (nM)	33
urine	A X	Affinity-gel-SPE	HPLC-MS	0.08 0.12	34
urine	A G	Affinity-gel-SPE	CE-MS	0.0194(nmol/mL) 0.0995(nmol/mL)	35
urine	A G UA X	MWCNTs/SiO_2-SPE	HPLC-DAD	0.00122 0.00202 0.00032 0.00228	this work

[a] DSPE: dispersive solid phase extraction; [b] SPE: solid phase extraction; [c] CE: capillary electrophoretic

Conclusion

Multi-walled carbon nanotubes coated silica microsphere has been synthesized by covalently bonding. SPE coupled with HPLC-DAD method for the simultaneous quantification of A, G, UA and X in human urine was developed. Method validation has been demonstrated by a series of experiments for linearity, sensitivity, precision, salt effect, recovery and stability. Moreover, by the evaluation of static, dynamic adsorption

experiments, adsorption kinetics and adsorption isotherms, the adsorption mechanisms between MWCNTs/SiO_2 and nucleobases and nucleosides were clarified, which were mainly attributed to the chemical interaction of π–π conjugations and hydrogen bond actions. This method has been shown to be suitable for the analysis of A, G, UA and X because of its high sensitivity, accuracy and selectivity.

Acknowledgments

This research was financially supported by the National Natural Science Foundation of China (NSFC No.21205126) and Important Technology Plan Projects of Lanzhou City (2012-2-66). Thanks are due to Group 501 in Lanzhou Institute of Chemical Physics, ACS for assistance with the experiments.

Notes and references

[a] *Key Laboratory of Chemistry of Northwestern Plant Resources and Key Laboratory for Natural Medicine of Gansu Province, Lanzhou Institute of Chemical Physics, Chinese Academy of Sciences, 18 Tianshui Middle Road, Lanzhou, China. Fax:+86 931 8277088; Tel:+86 931 4968248; E-mail: didl@licp.cas.cn*

[b] *Key Laboratory of Chemistry and Quality for Traditional Chinese Medicines of the College of Gansu Province, Department of Pharmacy, Gansu College of Traditional Chinese Medicine, 35 Dingxi East Road, Lanzhou, China.*

1. J.K. Nicholson, J.C. Lindon, E. Holmes, *Xenobiotica*, 1999, 11, 1181–1189.
2. C.M. Jabs, P. Neglen, B. Eklof, E.J. Thomas, *Clin. Chem.*, 1990, 36, 81-87.
3. T. Yamamoto, H. Koyama, M. Kurajoh, T. Shoji, Z. Tsutsumi, Y. Moriwaki, *Clin. Chim. Acta*, 2011, 412, 1712-1724.
4. Y. Liu, X.M. Sun, D.L. Di, J.X. Quan, J. Zhang, X.F. Yang, *Clin. Chim. Acta.*, 2011, 412, 2132-2140.
5. J. Czarnecka, M. Ciéslak, K. Michał, *J. Chromatogr. B*, 2005, 822, 85-90.
6. T. Henriksen, P.R. Hillestrøm, H.E. Poulsen, A. Weimann, *Free Radic. Biol. Med.*, 2009, 47, 629-635.
7. L.R. Bushman, J.J. Kiser, J.E. Rower, B. Klein, J.H. Zheng, M.L. Ray, P.L. Anderson, *J. Pharm. Biomed. Anal.*, 2011, 56, 390-401.
8. P. Liu, Y.Y. Li, H.M. Li, D.J. Wan, Y.J. Tang, *Anal. Chim. Acta*, 2011, 687, 159-167.
9. E. Szymánska, M.J. Markuszewski, K. Bodzioch, R. Kaliszan, *J. Pharm. Biomed. Anal.*, 2007, 44, 1118-1126.
10. Y. Inoue, W. Kamichatani, M. Saito, Y. Kobayashi, A. Yamamoto, *Chromatographia*, 2011, 73, 849-855.
11. W.Z. Wang, B. Feng, X. Li, P.Y. Yin, P. Gao, X.J. Zhao, X. Lu, M.H. Zheng, G.W. Xu, *Mol. BioSyst.*, 2010, 6, 1947-1955.
12. X.L. Dong, J.S. Cheng, J.H. Li,Y.S. Wang, *Anal. Chem.*, 2010, 82, 6208-6214.
13. A. Plewa,S.I. Yusa,M. Szuwarzyński, K. Szczubiałka, Y. Morishima, M. Nowakowska, *J. Med. Chem.*, 2012, 55, 8712-8720.
14. D. Jégourel, R. Delépée, F. Breton, A. Rolland, R. Vidal, L.A. Agrofoglio, *Bioorg. Med. Chem.*, 2008, 16, 8932-8939.
15. S. Scorrano, L. Longo, G. Vasapollo, *Anal. Chim. Acta*, 2010, 659, 167-171.
16. M. Soylak, Y.E. Unsal, *J. AOAC Int.*, 2011, 94, 1297-1303.
17.S.G. Ozcan, N. Satiroglu, M. Soylak, *Food Chem. Toxicol.*,2010, 48, 2401-2406.
18. E.M. Soliman, H.M. Marwani, H.M. Albishri, *Environ. Monit. Assess.*, 2013, 185, 10269-10280.
19. S. López-Feria, S. Cárdenas, M. Valcárcel, *J. Chromatogr. A*, 2009, 1216, 7346-7350.
20.P.F. Yu, Q. Wang, X.F. Zhang, X.S. Zhang, S. Shen, Y. Wang, *Anal. Chim. Acta*, 2010, 678, 50-55.
21. P. Viñas, I. López-García, M.B. Bravo, M. Hernández-Córdoba, *Anal. Bioanal. Chem.*, 2011, 401, 1393-1399.
22. Y.B. Luo, G.T. Zhu, X.S. Li, B.F. Yuan, Y.Q. Feng, *J. Chromatogr. A*, 2013, 1299, 10-17.
23.Y.B. Luo, Q.W. Yu, B.F. Yuan, Y.Q. Feng, *Talanta*, 2012, 90, 123–131
24. L. Wang, J.M. Liu, P. Zhao, Z.W. Ning, H.L. Fan, *J. Chromatogr. A*, 2010, 1217, 5741-5745.
25. J.G. Hu, Z.X. Wang, W. Zhang, Z.J. Xu, Y.Q. Wu, Z.Y. Zhu, X.F. Duan, *Carbon*, 2006, 44, 1581-1583.
26. T. Fujigaya, J.T. Yoo, N. Nakashima, *Carbon*, 2011, 49, 468-476.
27. M. Bottini, L. Tautz, H. Huynh, E. Monosov, N. Bottini, M.I. Dawson, S. Bellucci, T. Mustelin, *Chem. Commun.*, 2005, 41, 758-760.
28. B. Akdim, R. Pachter, P.N. Day, S.S. Kim, R.R. Naik, *Nanotechnol.*, 2012, 23, 165703.
29. H.M. Wang, A. Ceulemans, *Physical Review B*, 2009, 79, 195419.
30. M. Calero, G. Blázquez, M.A. Martín-Lara, *J. Chem. Eng. Data*, 2011, 56, 3053-3060.
31. Y.F. Liu, Q.Q. Bai, S. Lou, D.L. Di, J.T. Li, M. Guo, *J. Agric. Food. Chem.*, 2012, 60, 1555-1566.
32. H.B. He, Y.R. Sun, B. Li, Q.W. Yu, T.L. Wang, Y.Q. Feng, *Anal. Methods*, 2013, 5, 1435-1441.
33. Y.Q. Jiang, Y.F. Ma, *Anal. Chem*, 2009, 81, 6474-6480.
34. W. Struck, D. Siluk, A. Yumba-Mpanga, M. Markuszewski, R. Kaliszan, M.J. Markuszewski, *J. Chromatogr. A*, 2013, 1283, 122-131.
35. S. Wang, X.P. Zhao, Y. Mao, Y.Y. Cheng, *J. Chromatogr. A*, 2007, 1147, 254-260.

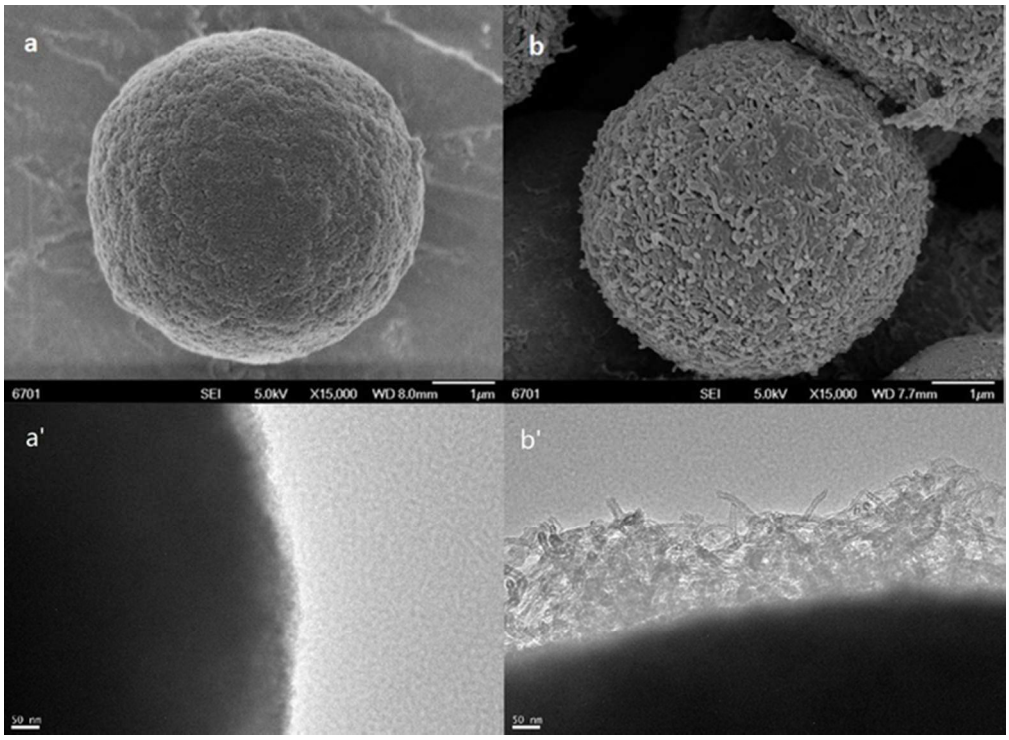

Figure 1: SEM and TEM micrographs of adsorptions.SEM: bare silica microspheres (a) and MWCNTs/SiO2 (b); TEM: bare silica microspheres (a') and MWCNTs/SiO2 (b')
58x42mm (300 x 300 DPI)

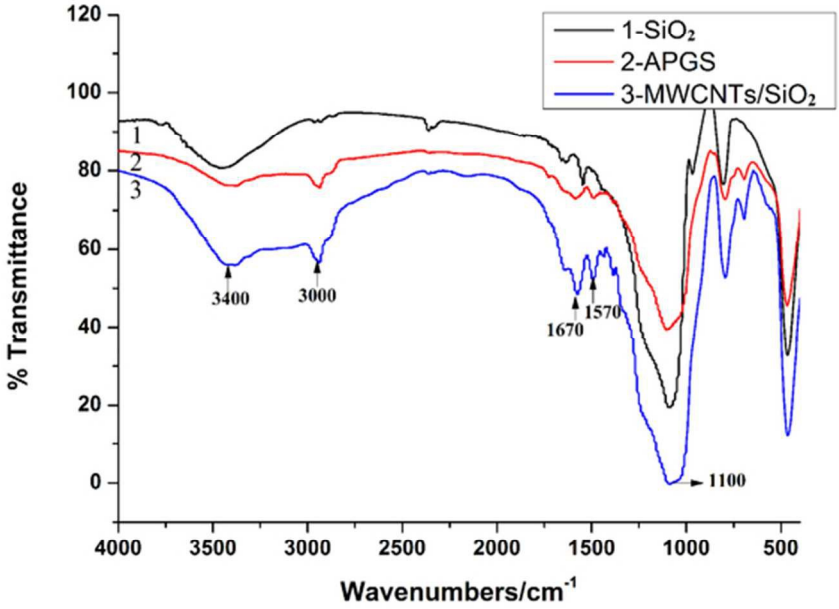

Figure 2: FTIR spectra of pristine silica microspheres, APGS and MWCNTs/SiO2. 1: SiO2; 2: APGS; 3: MWCNTs/SiO2.
56x39mm (300 x 300 DPI)

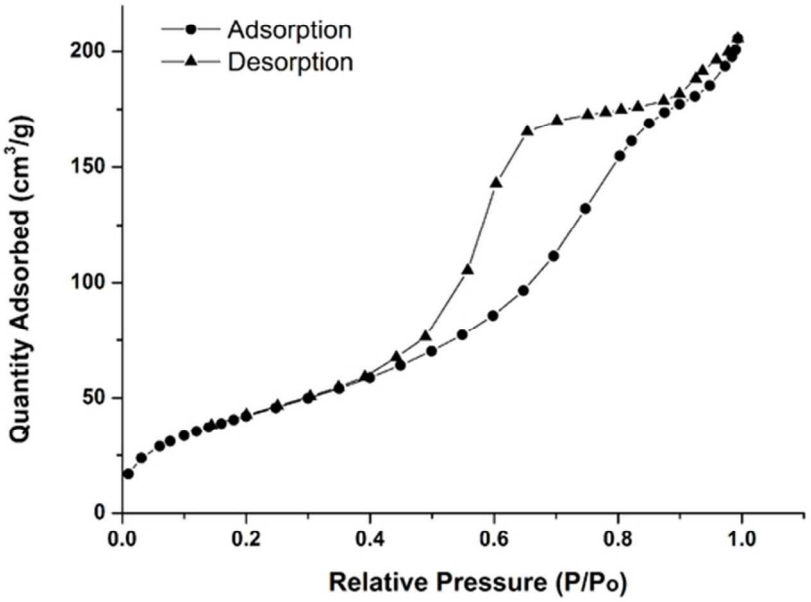

Figure 3: Nitrogen adsorption/desorption isotherms of MWCNTs/SiO2 microsphere.
56x39mm (300 x 300 DPI)

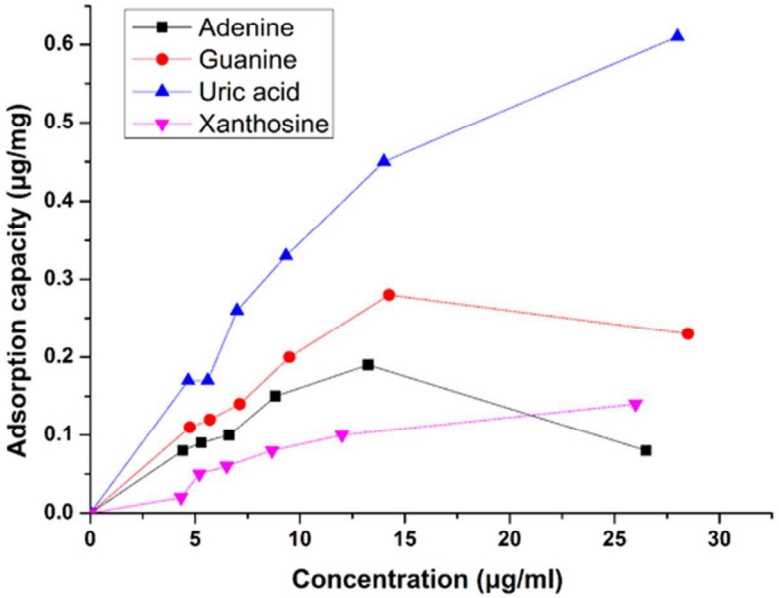

Figure 4: The adsorption capacities of A, G, UA and X.
56x39mm (300 x 300 DPI)

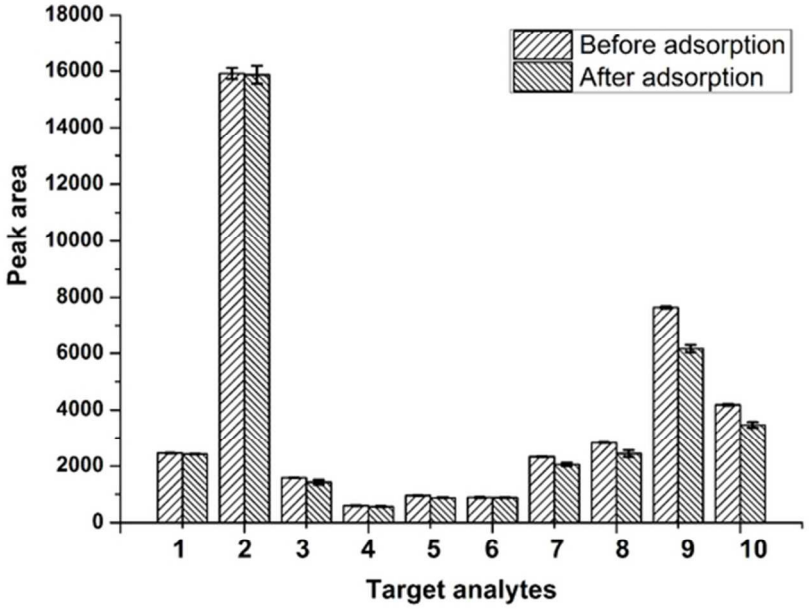

Figure 5: Adsorption characters of ten nucleobases and nucleosides. (The concentration are as follows, 1. uracil: 0.07 mg/ml; 2. xanthine: 0.27 mg/ml; 3. hypoxanthine: 0.05 mg/ml; 4. uridine: 0.03 mg/ml; 5. inosine: 0.07 mg/ml; 6. guanosine: 0.04 mg/ml; 7. guanine: 0.04 mg/ml; 8.adenine: 0.06 mg/ml; 9.xanthosine: 0.17 mg/ml; 10. uric acid: 0.22 mg/ml).
56x39mm (300 x 300 DPI)

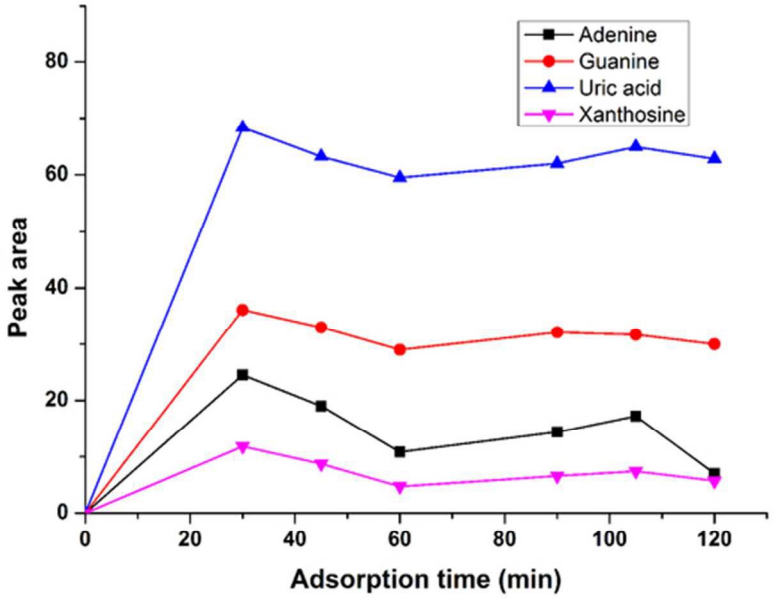

Figure 6: Effect of extraction time on the extraction efficiency. Sample solution, 2 mL of aqueous solution containing 2.5 µg/mL of A, 2.0 µg/mL of G,10.4 µg/mL of UA and 10 µg/mL of X. Extraction temperature was 30 oC; stirring speed was 100 rpm without addition of salt.
56x39mm (300 x 300 DPI)

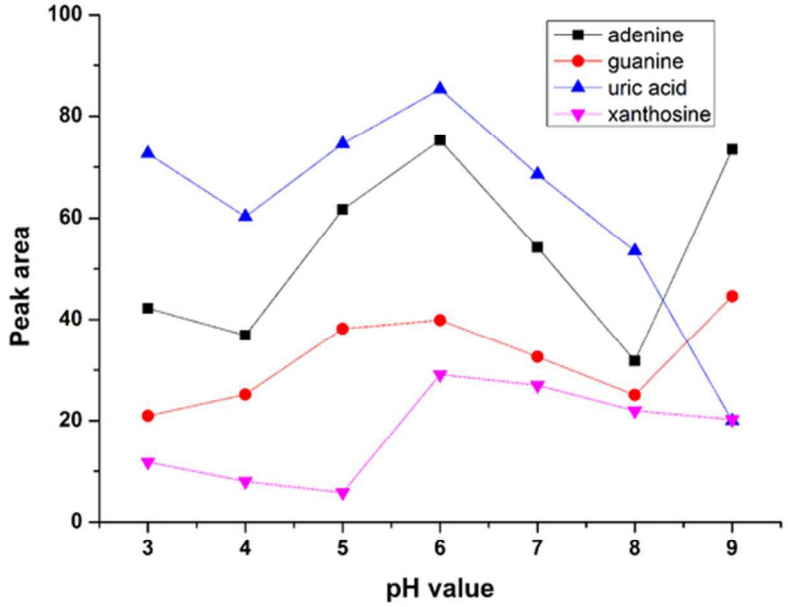

Figure 7: Effect of sample pH on the extraction efficiency of A, G, UA and X extracted with MWCNTs/SiO2-SPE. Sample solution, 3 mL of aqueous solution containing 4.2 µg/mL of A, 3.3 µg/mL of G, 17.3 µg/mL of UA and 16.8 µg/mL of X.
56x39mm (300 x 300 DPI)

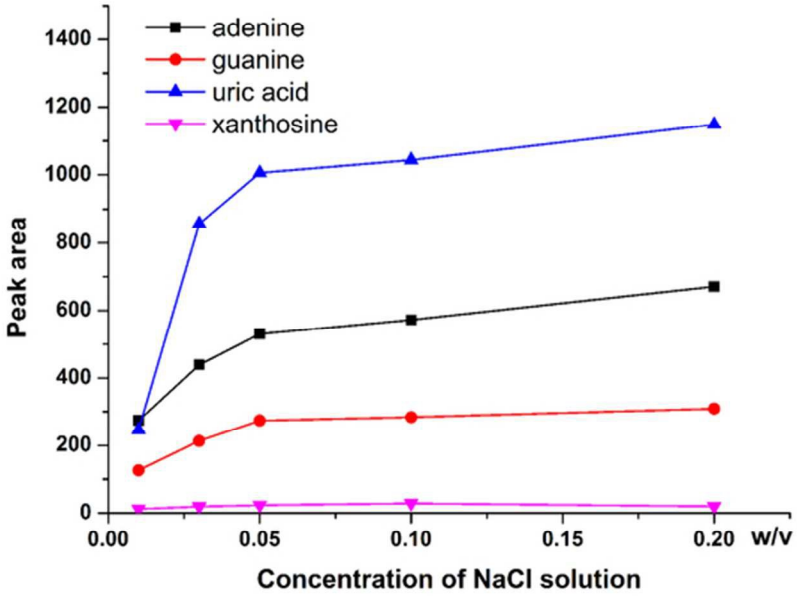

Figure 8: Effect of salt addition to the adsorption efficiency.
56x39mm (300 x 300 DPI)

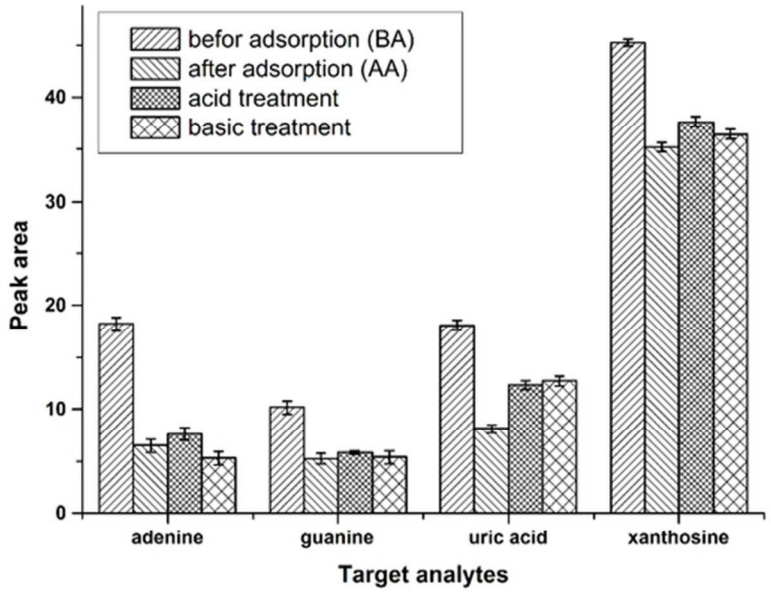

Figure 9: Evaluation of the stability of MWCNTs/SiO2 adsorbents under acid and/or basic environment.
56x39mm (300 x 300 DPI)

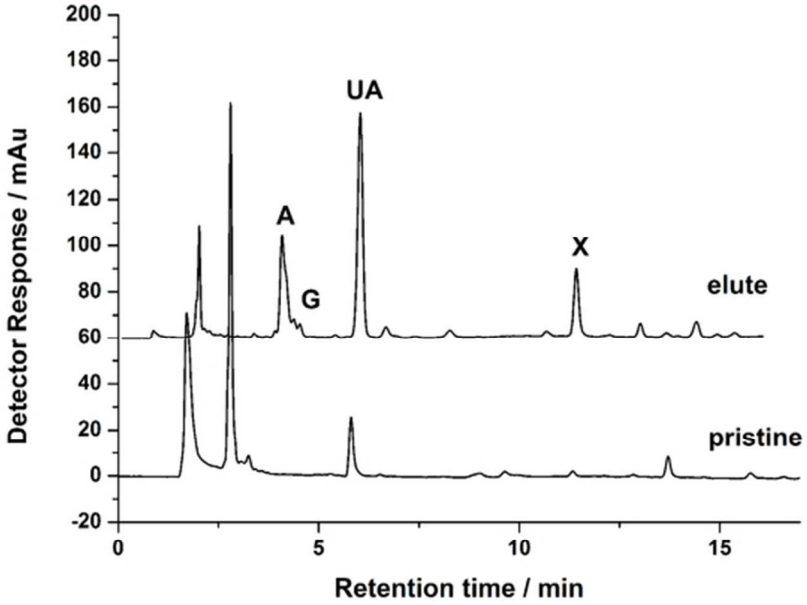

Figure 10: Chromatograms of pristine and elute solution of real urine sample.
56x39mm (300 x 300 DPI)

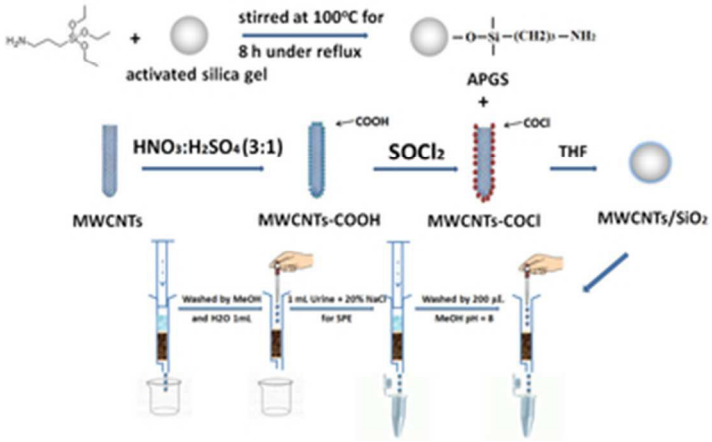

Nucleobases and nucleosides in human urine could be detected by new efficient and selective adsorbent of MWCNTs/SiO2 in human urine.
39x19mm (300 x 300 DPI)